nature medicine

SUPPLEMENTARY INFORMATION

https://doi.org/10.1038/s41591-018-0058-y

In the format provided by the authors and unedited.

Low-frequency cortical activity is a neuromodulatory target that tracks recovery after stroke

Dhakshin S. Ramanathan[1,2,3,4,5,11], Ling Guo[1,6,11], Tanuj Gulati[1,7,11], Gray Davidson[1,2,3], April K. Hishinuma[1,7], Seok-Joon Won[1,7], Robert T. Knight[8,9], Edward F. Chang[10], Raymond A. Swanson[1,7] and Karunesh Ganguly[1,7]*

[1]Neurology Service, San Francisco Veterans Affairs Medical Center, San Francisco, CA, USA. [2]Mental Health Service, San Francisco Veterans Affairs Medical Center, San Francisco, CA, USA. [3]Department of Psychiatry, University of California, San Francisco, San Francisco, CA, USA. [4]Mental Health Service, VA San Diego Health System, San Diego, San Diego, CA, USA. [5]Department of Psychiatry, University of California, San Diego, San Diego, CA, USA. [6]Neuroscience Graduate Program, University of California, San Francisco, San Francisco, CA, USA. [7]Department of Neurology, University of California, San Francisco, San Francisco, CA, USA. [8]Helen Wills Neuroscience Institute, University of California, Berkeley, Berkeley, CA, USA. [9]Department of Psychology, University of California, Berkeley, Berkeley, CA, USA. [10]Department of Neurosurgery, University of California, San Francisco, San Francisco, CA, USA. [11]These authors contributed equally: Dhakshin S. Ramanathan, Ling Guo, Tanuj Gulati. *e-mail: karunesh.ganguly@ucsf.edu

SUPPLEMENTARY FIGURES

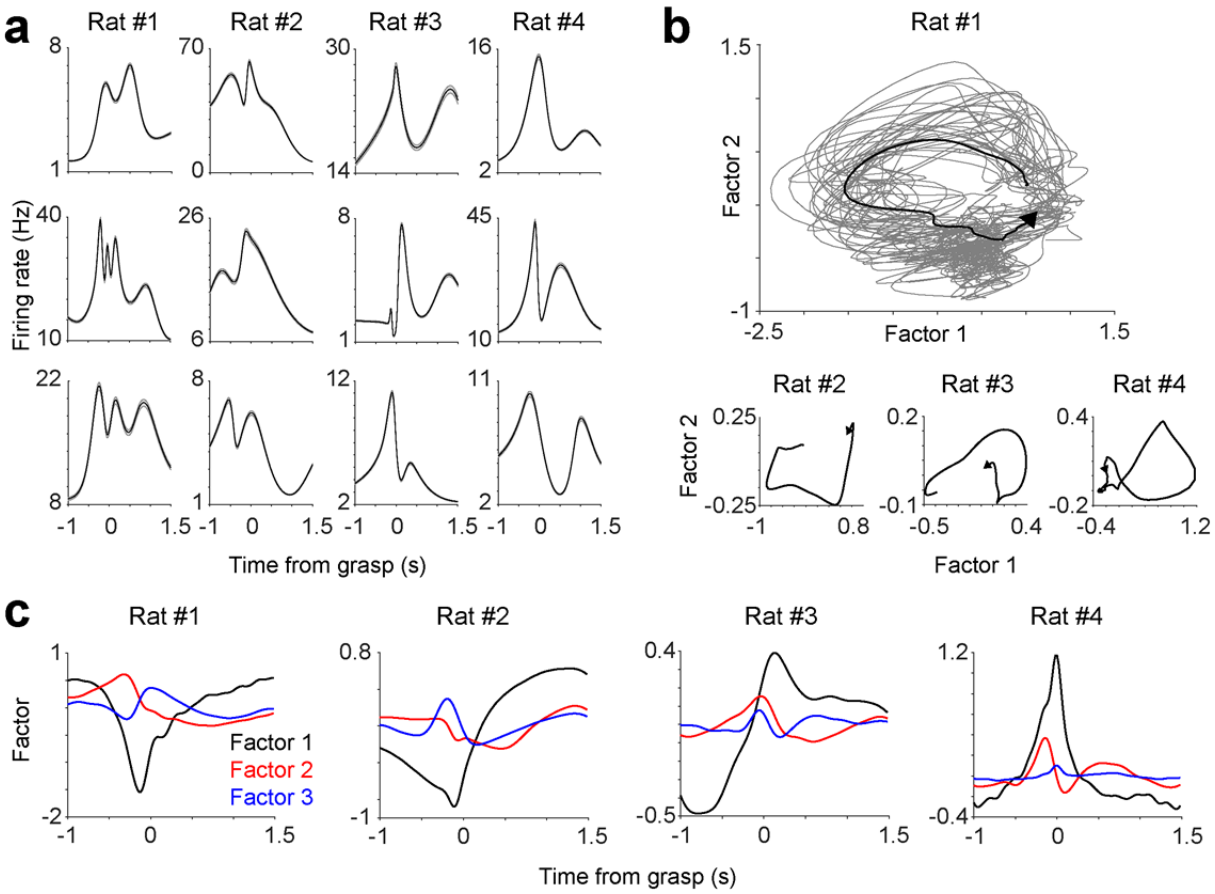

Supplementary Figure 1: Low frequency quasi-oscillatory dynamics in unit spiking during reaching in healthy rats. a. Examples of smoothed peri-event time histograms of single unit spiking from all 4 rats, showing multiphasic changes in firing rate relative to grasp onset. These are representative examples of unit firing and population dynamics were examined in subsequent panels. **b.** Neural population trajectory during reach, from -1s to +1.5 around grasp, calculated using gaussian process factor analysis (Yu et al., 1009; Cowley et al., 2013). Thick black line shows mean across all trials (n = 91, 145, 100 and 73 trials for rats 1-4 respectively), and grey lines in top plot represent 30 example trials. **c.** Top 3 factors from GPFA, in terms of variance accounted for, from all 4 rats showing multi-phasic changes in population neural activity during reaching.

Yu, B. M. *et al.* Gaussian-process factor analysis for low-dimensional single-trial analysis of neural population activity. in *Advances in Neural Information Processing Systems 21* (eds. Koller, D., Schuurmans, D., Bengio, Y. & Bottou, L.) 1881–1888 (Curran Associates, Inc., 2009).

Cowley, B. R. *et al.* DataHigh: graphical user interface for visualizing and interacting with high-dimensional neural activity. *J. Neural Eng.* **10,** 066012 (2013).

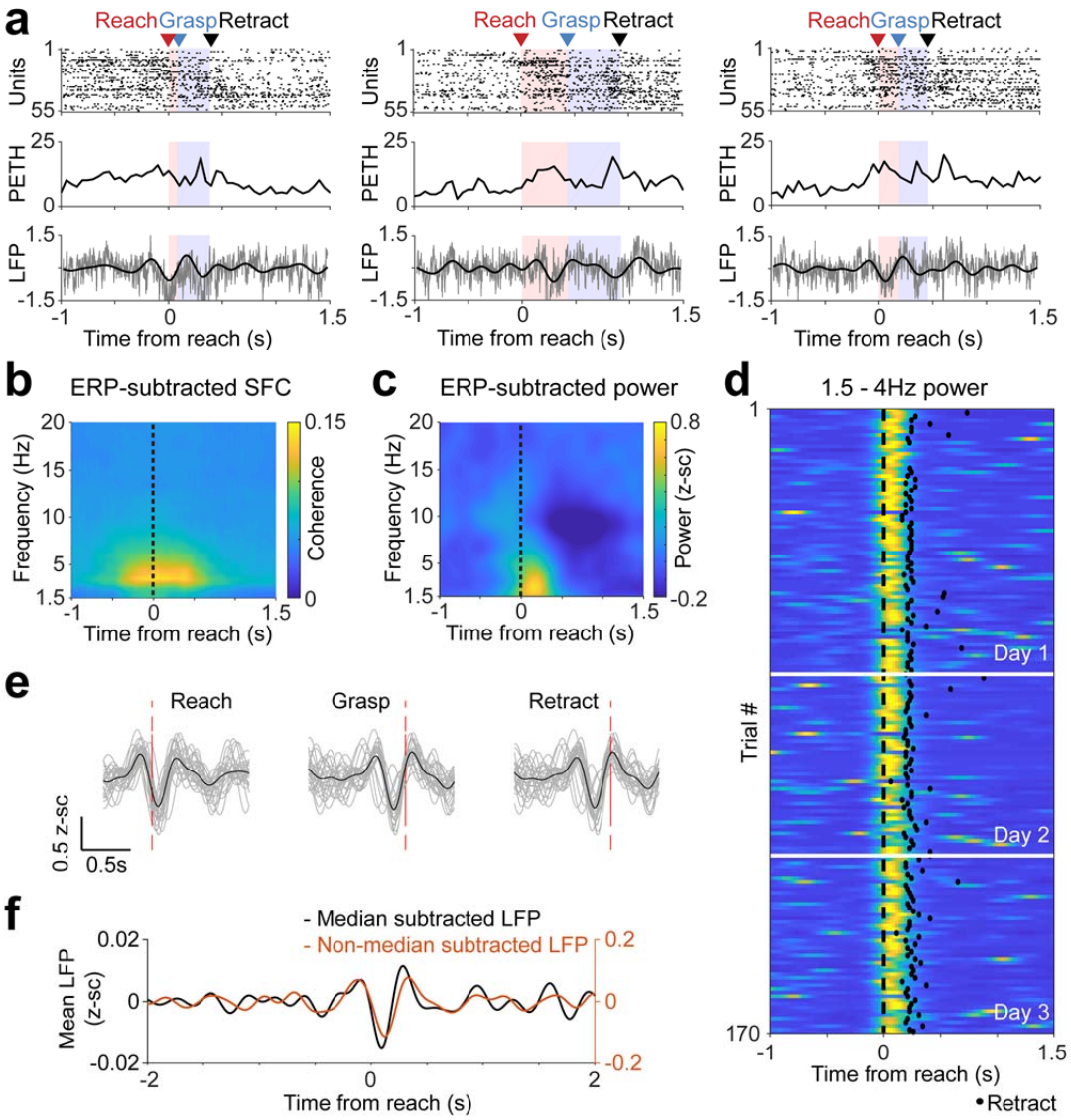

Supplementary Figure 2: Task-related LFO in healthy rats. **a.** Example single trials from healthy rodents during reaching, showing quasi-oscillatory activity in both unit spiking and LFP. Top: spike raster of all units in example trial, middle: population peri-event time histogram for all spikes shown on top, bottom: raw LFP in gray and LFP filtered from 1.5 – 4 Hz in black from an example channel. These trials are representative examples of trials that show high SFC and power, as quantified in Fig 1. **b-c.** Mean spike-field coherence (n = 171 units) and LFP (n = 118 channels) spectrograms from all 4 animals after the mean evoked potential (ERP) was subtracted. **d.** 1.5-4Hz LFP power of single trials over 3 recording sessions (1 session per day) from an example channel. Similar patterns of power increases can be observed across trials/days. **e.** Example data from one animal demonstrating single-trial LFP signals from 20 trials, filtered from 1.5-4Hz. There was striking phase-locking to behavioral markers. **f.** Comparison of the median-referenced and unreferenced LFP signal (mean activity across all 118 channels from 4 healthy animals). Other than the exact amplitude of the signal, there was no observed difference in the temporal features. Data presented in this paper primarily used from median referenced data.

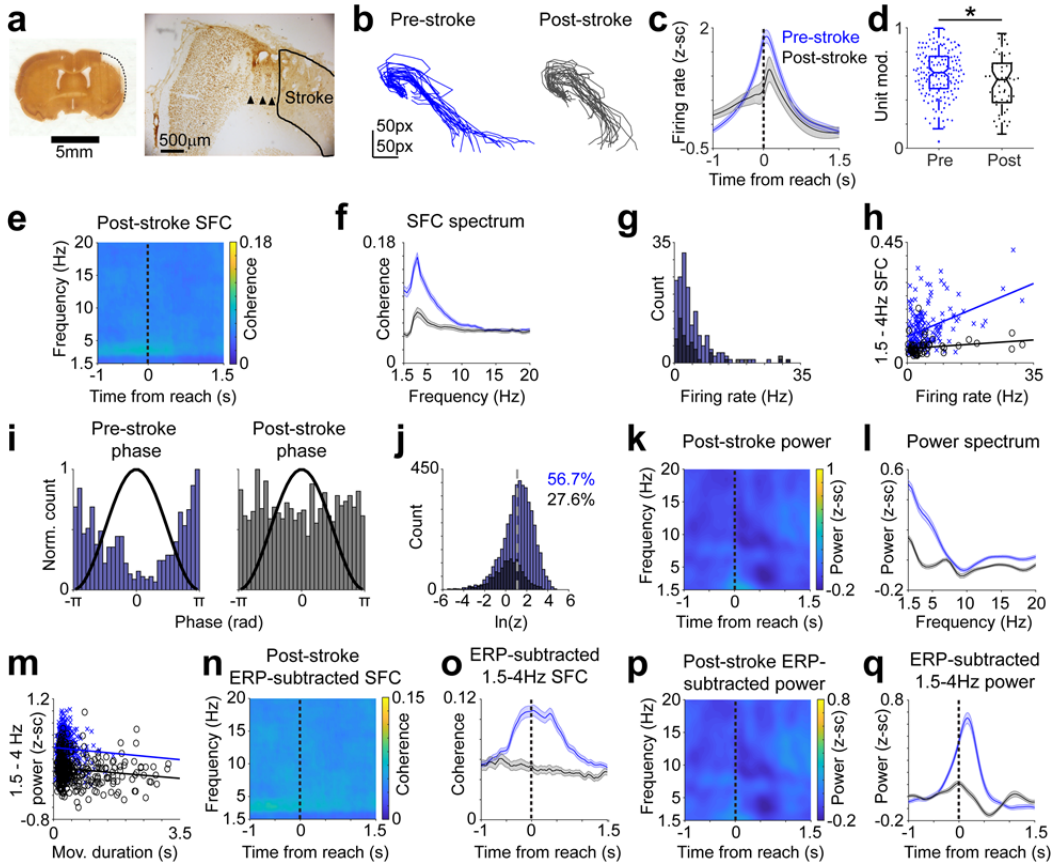

Supplementary Figure 3: Reduction in LFO after stroke. a. Left: coronal histology section showing lesion caused by MCA stroke. Right: Magnified coronal section showing electrode tracks (black arrows) next to stroke lesion. We performed a similar histological analysis in 4 animals to verify that there was a lesion from stroke. **b.** Example paw trajectories during reach in the same animal before and after MCA stroke (25 trials each). Color code is maintained for the rest of the figure. Axis refers to both plots. px=pixel. **c.** Mean z-scored firing rate of all units pre- (n = 171) and post- (n = 53) stroke from 4 rats. Shaded area represents SEM. **d.** Unit modulation decreased after stroke (mixed-effects model t(221) = 2.51, *p = 0.0128). Each dot represents modulation of one unit. Center line in boxplot is median and the tops and bottoms are the 25th and 75th percentiles. Whiskers indicate range excluding outliers (>1.5 times interquartile range). **e.** Mean SFC spectrogram after stroke (n = 53 units from 4 rats). **f.** Mean SFC spectrum –0.25 to 0.75s around reach (n = 171 pre and 53 post stroke, from 4 rats). Shaded area shows SEM. **g.** Firing rate histograms of units before (n = 171) and after (n = 53) stroke. There was no significant difference in mean firing rate (across both baseline and task periods) of units pre- and post-stroke (2-sided rank-sum test, z = 0.48, p = 0.63). **h.** Scatter of 1.5-4Hz task-related SFC (-0.25 to 0.75s around reach) versus mean firing rate of each unit. Least squares lines were fitted for units pre- (n = 171) and post- (n = 53) stroke. There is a reduction in low frequency SFC even when comparing units with similar firing rates before and after stroke. **i.** Histograms of spike phases (-0.25 to 0.75 around reach) relative to 1.5-4Hz LFP for example units pre- and post-stroke. **j.** Histogram of natural log of Rayleigh's z (from Rayleigh's test of circular uniformity) in all spike-LFP pairs pre (n = 4700) and post stroke (n = 1263). Values greater than grey dotted line (ln(z)>1.09) have p-values <0.05. Numbers indicate the percentage of spike-LFP pairs with significantly non-uniform phase histograms. **k.** Mean post-stroke power spectrogram (n = 117 channels from 4 rats). **l.** Mean power spectrum –0.25 to 0.75s around reach (n = 117 channels from 4 rats). Shaded area is SEM. **m.** Scatter of 1.5-4Hz task-related power versus movement duration (from reach onset to retract) for each trial from all 4 animals before (n = 389 trials) and after (n = 355) stroke, fitted with least squares lines. Power and duration were not correlated (Pearson's correlation r = -0.0765, p = 0.132 pre-stroke and r = -0.0888, p = 0.0947 post-stroke) and there was a reduction in low frequency power post-stroke regardless of movement duration. **n-o.** Mean SFC after mean evoked potential (ERP) was subtracted (53 units from 4 rats). **o.** Mean 1.5-4Hz SFC before (n = 171) and after (n = 53) ERP was subtracted. Shaded area is SEM. **p.** Mean LFP power spectrogram after ERP subtraction (n = 117

channels). **q.** Mean 1.5-4Hz LFP power before and after stroke (n = 101 paired channels from 4 rats). Shaded area is SEM.

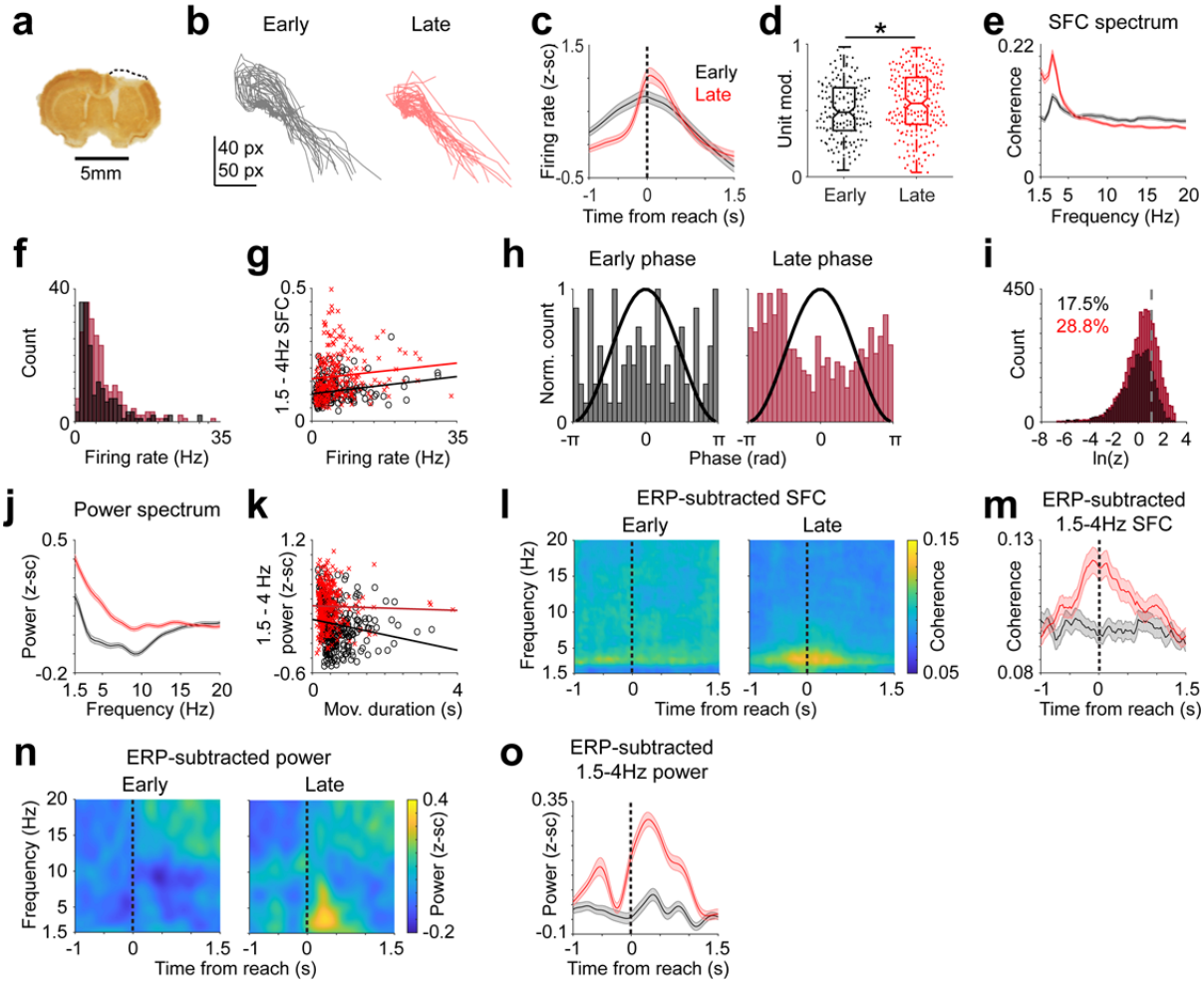

Supplementary Figure 4. Restoration of LFO in perilesional cortex with rehabilitation. a. Coronal histology section showing lesion caused by photothrombotic stroke. We performed a similar histological analysis in 6 animals to verify that there was a lesion from stroke. **b.** Example early (first 25 trials in first session) and late (last 25 in last session) paw trajectories in the same animal. px=pixel. Color code is maintained for the rest of the figure **c.** Mean z-scored firing of all units in all 6 animals in early (first, n = 170) and late (last, n = 219) sessions. Shaded area is SEM. **d.** Units became more task-modulated from early (n = 170) to late (n = 219) rehabilitation sessions (mixed-effects model t(387) = 3.30, *p = 0.00104). Each dot represents one unit. Center line in boxplot is median and the tops and bottoms are the 25th and 75th percentiles. Whiskers indicate range excluding outliers (>1.5 times interquartile range). **e.** Mean SFC spectrum across all units in early (n = 170) and late (n = 219) sessions from –0.25 to 0.75 around reach. **f.** Histogram of mean firing rate (across both baseline and task periods) of all units in early (n = 170) and late (n = 219) sessions. There was a significant increase in firing rate of units from early to late (2-sided rank-sum test, z=3.96, p=7.61e-5). **g.** Scatter of 1.5-4Hz SFC versus firing rate for each unit (n = 170 early and n = 219 late), with fitted least squares lines. Units show higher low-frequency SFC in late compared to early sessions, even when comparing units with similar firing rates. **h.** Histograms of spike phases (-0.25 to 0.75 around reach) relative to 1.5-4Hz LFP for 2 example units in early and late rehabilitation sessions. **i.** Histogram of natural log of Rayleigh's z (from Rayleigh's test of circular uniformity) in all spike-LFP pairs in early (n = 3649 pairs) and late sessions (n = 5675). Values greater than grey dotted line (ln(z)>1.09) have p-values <0.05. Numbers indicate the percentage of spike-LFP pairs with significantly non-uniform phase histograms. **j.** Mean power spectrum across all channels (n = 176 channels from 6 rats) in early (first 50) and late (last 50) trials, from –0.25 to 0.75s around reach. Shaded area is SEM **k.** Scatter of 1.5-4Hz task-related power versus movement duration for each trial (n = 300 trials for both early and late, from 6 rats), with fitted least squares lines. Low frequency power increased from early to late trials, even when comparing trials with similar movement duration. **l-m.** Mean ERP-subtracted SFC spectrograms early (n = 170) and late (n = 219). Shaded area is in m SEM. **n-o.** Mean ERP-subtracted LFP power spectrograms (n = 176 channels from 6 rats). Shaded area is in o SEM.

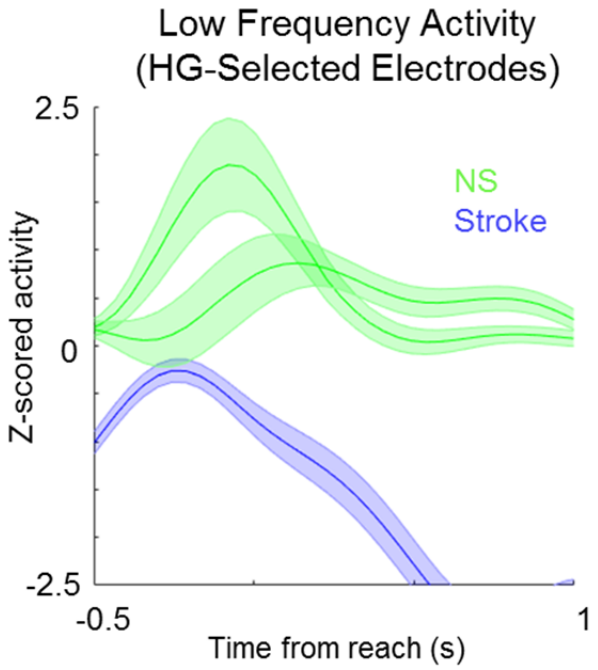

Supplementary Figure 5: Functional selection of electrodes. We used a blind/automated approach of selecting electrodes based on significant increases in high-gamma (70 – 150 Hz) activity. For each channel, we quantified the 95% CI in the high-gamma band (70 – 150 Hz). If the mean activity between -300 ms before and 100 ms after reach was greater than the 95% CI, we included that channel in our analysis. Using this method, the low-frequency activity in the stroke subject was significant lower than the healthy subjects activity during the time-points of interest (-300 to + 300 msec after reach). NS1 (n = 8 electrodes), NS2 (n = 7 electrodes), SS1 (n = 103 electrodes). Using this approach, we still found a significant increase in LFO in NS1/NS2($t(7) = 4.57$, $p = 0.003$ for NS1; $t(6) = 2.46$, $p = 0.049$ for NS2) and significant a reduction in LFO in SS ($t(102) = -4.18$, $p = 6.1e\text{-}5$). As before, we assessed the overall effect of stroke by performing an ANOVA across all channels from stroke vs. healthy subjects, with subject included as a fixed effect in the model; the overall model was significant ($F(2,115) = 8.08$, $p = 0.001$; with a highly significant effect of stroke ($F(1,115) = 15$, $p = 1.82e\text{-}4$). All subjects showed the expected significant increase in high-gamma activity ($t(7) = 4.21$, $p = 0.004$ for NS1; $t(6) = 5.82$, $p = 0.001$ for NS2; and $t(102) = 21.3$, $p = 2.14e\text{-}39$) for the stroke subject, demonstrating our technique for electrode selection was effective at selecting channels with high-gamma activity, which is widely thought to reflect local spiking activity.

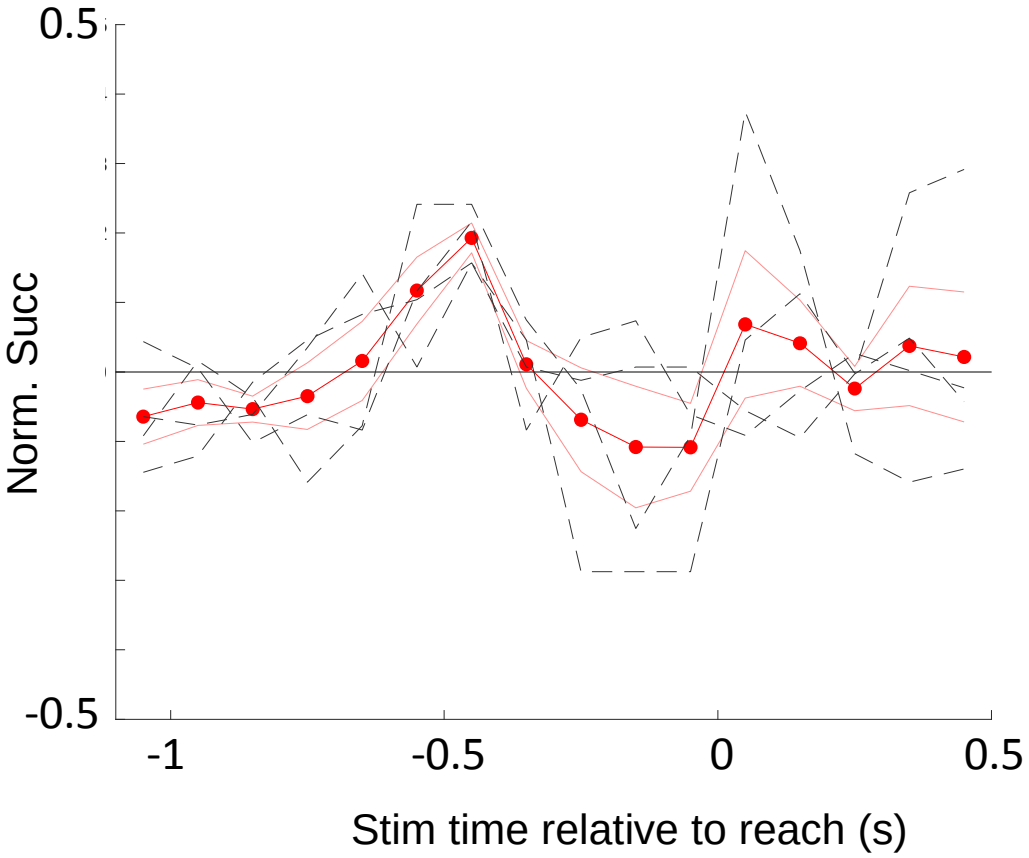

Supplementary Figure 6: Single animal data of brief-stimulation paradigm. Dark red line represents mean, variance shown with red shading, each of the gray dotted lines are the individual 4 animal traces. Across animals, there was a consistent increase in performance when stimulation occurs between -0.5 and -0.4s relative to reach onset.